SUPPLEMENT No. 409

Huss Mikael: Wave loads on visor attachments.

MV ESTONIA Accident Investigation. Internal report 1995 - 1997.

MV ESTONIA Accident Investigation
Internal Report
1995-1997

Wave loads on visor attachments

by
Mikael Huss

Introduction

The distribution of wave induced forces at the attachments of the bow visor has been estimated by using equilibrium equations and assumptions of relative distribution and direction of forces. The external loads have been taken from an estimated range of maximum wave forces and moments during the last 30 minutes before the accident, and are based on the model test at SSPA Maritime Dynamic Laboratory, (MDL).

1 Estimate of maximum wave loads for the accident condition

A probable range of maximum forces and moments for the accident condition has been evaluated from the MDL test for 150° heading, 14.5 knots and a (measured) significant wave height of 4.51 m. The evaluation has been done in three steps:

- Approximate probability distribution curve fit in the figures of SSPA report 7524-appendix
- Calculation of maximum loads during 30 minutes of exposure for a confidence interval of 90% based on the approximate distributions
- A reduction by 30% on forces and 50% on moment levels to make them correspond to a significant wave height of 4.0-4.1 m as is now assumed to be the most probable condition at the time of the accident.

Probability distribution of measured wave loads

The measured dynamic wave forces and moments about the hinge axis/centreline position are presented in SSPA Report 7524 as curves of ln(-ln(exceedance probability) versus ln(load level). A linear curve fit have been made to these figures which equals an assumption of Weibull-distributed load levels. The numerical simulations performed at VTT indicates that this assumption is valid for the vertical forces even down to very low levels of probability. This also holds for the measured forces from model tests. However, the upper tail of the measured wave induced moments seem to deviate from an ordinary Weibull distribution. This can partly be explained by the non-linearity between forces and moments due to the visor geometry, but there could also bee some influence from the wave conditions generated at the tests, where some of the larger waves were extremely steep with significantly higher crests than troughs. The highest values of the Y-moment (opening moment) have therefore been disregarded in the linear curve fit.

The SSPA plots with the corresponding linear curve fit are shown in Figures 1.1-1.5. The Z-moment distribution was not possible to evaluate directly from this test series.

A summary of the parameters of the fitted distributions is given in the table, Figure 1.6.

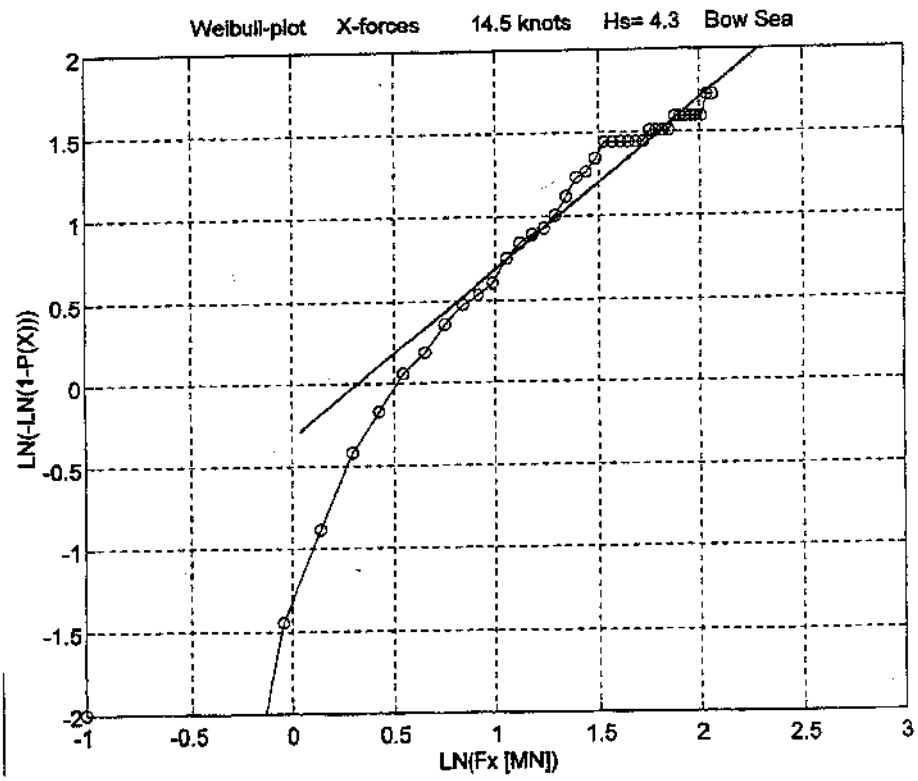

Figure 1.1 X-forces as measured and with Weibull-distribution curve fit

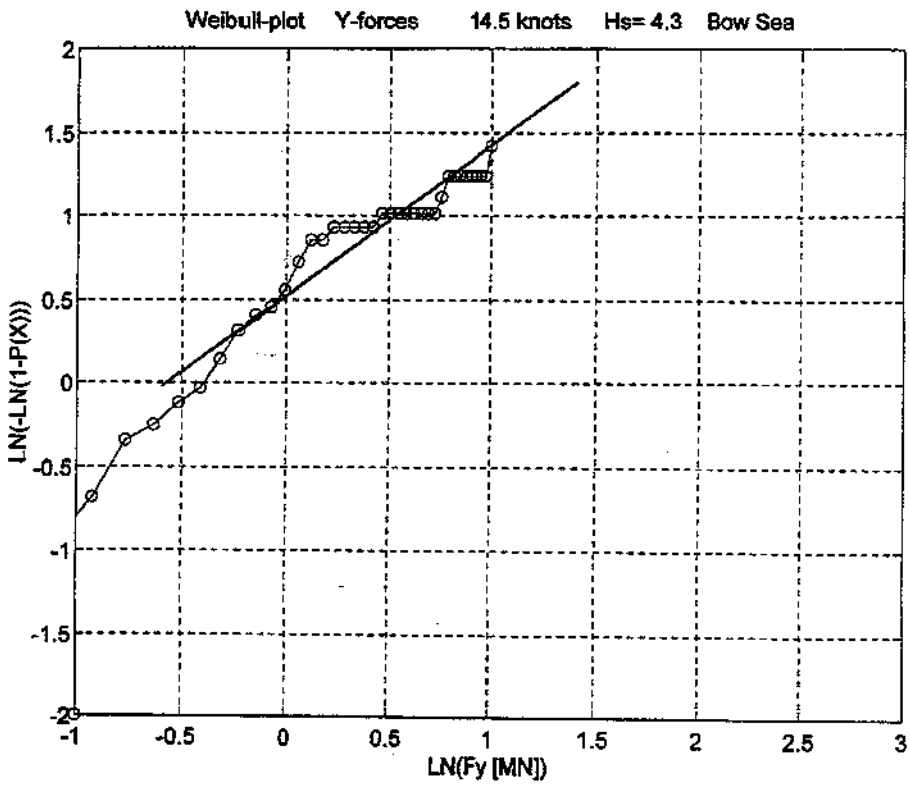

Figure 1.2 Y-forces as measured and with Weibull-distribution curve fit

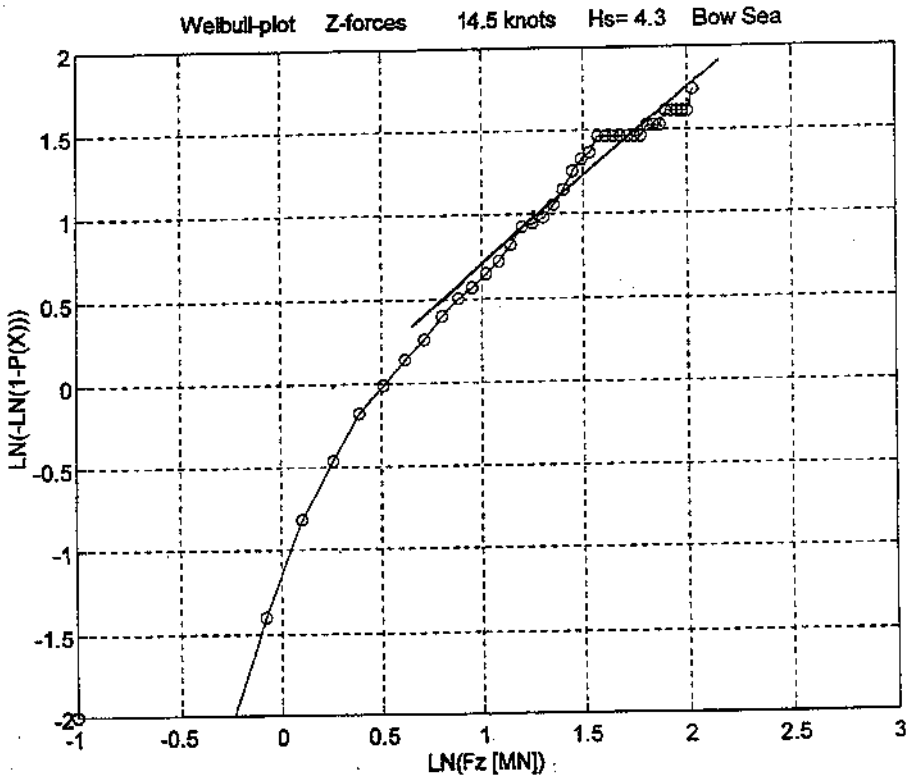

Figure 1.3 Z-forces as measured and with Weibull-distribution curve fit

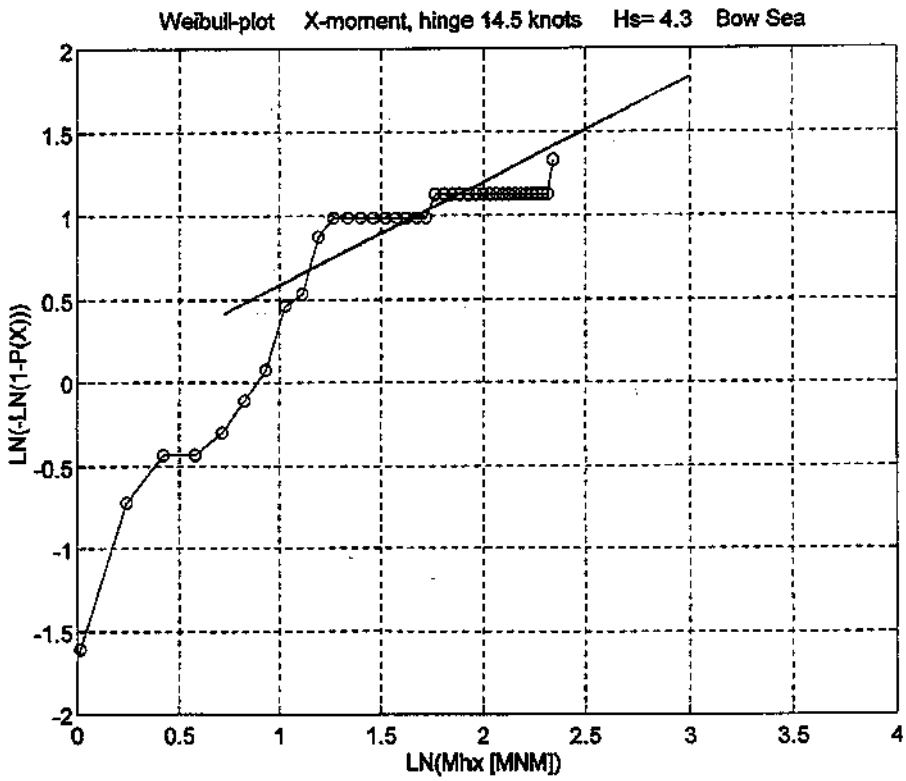

Figure 1.4 X-moments as measured and with Weibull-distribution curve fit

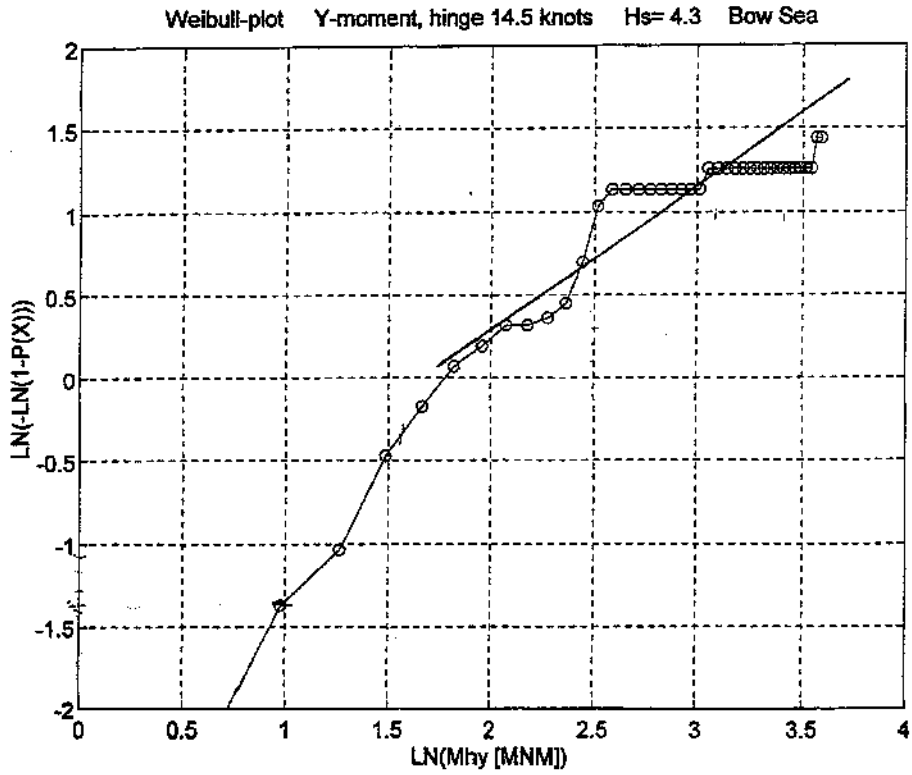

Figure 1.5 Y-moments as measured and with Weibull-distribution curve fit

Exceedance distributions and extreme value distributions for model test condition

The cumulative probability distributions corresponding to the linear curve fit of Figures 1.1-1.5 is expressed as:

$$F(x) = 1 - e^{-(x/b)^k}$$

where b and k are the parameters of the Weibull distribution.

The risk r to exceed a certain level x_r among n values is expressed by an extreme-value distribution defined from the basic cumulative distribution:

$$r = 1 - (F(x_r))^n$$

and the extreme level associated with a certain risk can be written

$$x_r = b(-\ln(1-(1-r)^{\frac{1}{n}}))^{\frac{1}{k}}$$

The estimated range of maximum wave loads are here based on 30 minutes of exposure and on risk levels 0.05 - 0.95. The number of cycles n have been taken from the model test results by taking one sixth of the measured cycles during the 3h test series.

Load type	Cumulative prob. distr.		no. of	Maximum value during 30 minutes		
			load peaks	Exceedance	Most	Exceedance
[MN]	Weibull parameters			probability	Probable	probability
[MNm]	b	k	n	0.95		0.05
X-force	1.41	1.04	50	3.85	5.23	9.01
Y-force	0.58	0.93	11	0.85	1.49	3.53
Z-force	1.40	1.05	53	3.86	5.20	8.86
X-moment	1.00	0.60	8	1.28	3.39	14.88
Y-moment	5.11	0.81	11	7.97	15.04	40.71
Z-moment	not possible to evaluate from the report					

Figure 1.6 Summary of load level distributions for the model test condition Hs = 4.5 m

The k-parameter is a good indication of the degree of non-linearity. If the forces would have been linear to the relative motion between bow and wave surface, then k would have been around 2 (Rayleigh-distributed forces). The low number of load peaks and the low k-value gives for the chosen time and confidence interval a very wide span for the different load components and especially the moments. This illustrates clearly the large uncertainty in any estimate of the actual maximum wave load at the time of the accident.

Correction due to difference in wave height in tested and actual condition

The significant wave height was measured to 4.51 m during the long test series in bow sea at MDL. The actual wave condition at the time of the accident was according to the meteorological institutes lower, with Hs 4.0-4.1 m. It is very difficult to estimate the influence from wave height in this narrow range, 4.05-4.51 m, based on the different model tests. Instead is here used the results from the numerical simulations at VTT, since they include bow wave conditions with both 4.0 and 4.5 m significant wave height. For all simulated probability levels, the reduction on Z-force was about 25%. For comparable conditions in head sea, the model tests gave larger reductions than the simulations. Here is therefore used as a rough estimate a reduction of 30% on all forces to compensate for the difference in wave height between model test condition and the accident condition.

The reduction on moments have been estimated from the correlation between Z-forces and Y-moments according to Figure 1.7. The diagram includes the 13 highest forces and moments measured during the 3 h long model test series. For the Z-force levels in the range of 4-10 MN, a reduction with 30% will give an approximate reduction of about 50% on the moments. This reduction has here been used for all moments.

Figure 1.8 shows the range of probable maximum forces and moments for the accident condition. The Z-moment range has been estimated only based on the maximum measured value.

It must be noted that when these values are used in the analysis of the visor attachment loads, Z-force and Y-moments are reduced with the weight of the visor (about 0.6 MN and 3.0 MNm)

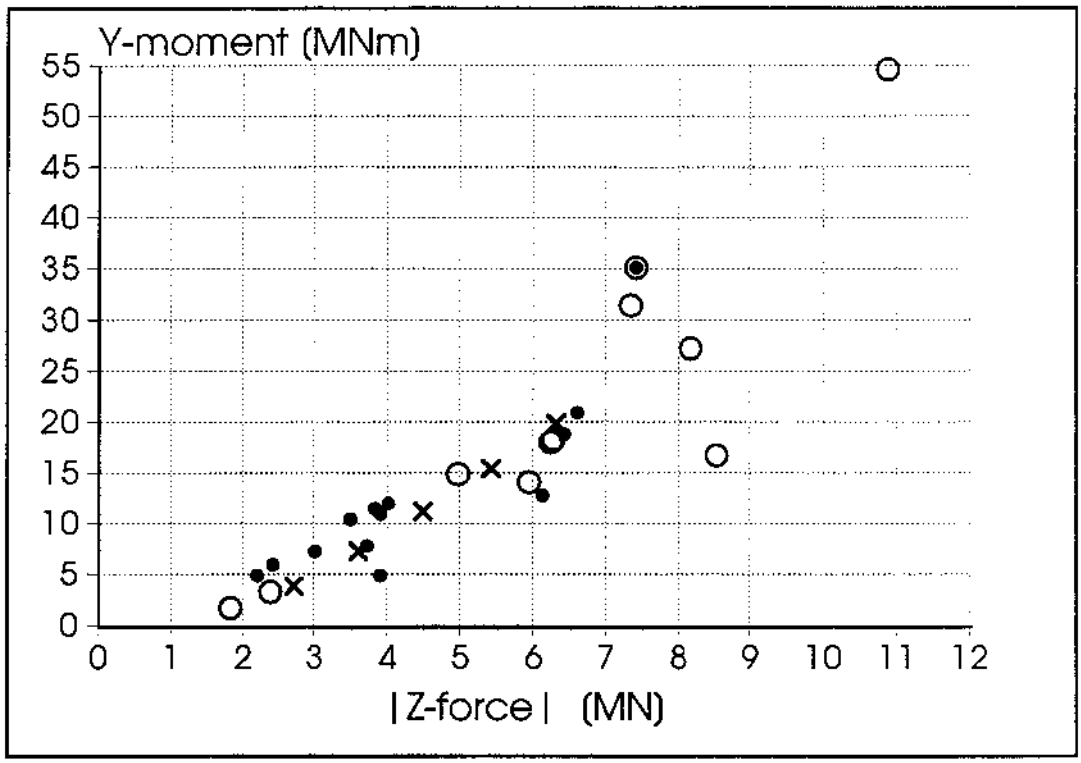

Figure 1.7 Correlation between Z-force and Y-moment, as measured at model tests
Filled spots show the 13 highest wave loads in Hs = 4.5m/V = 14.5 kn
Rings shows the single highest value from all different test series.
The 5 cross show the example load levels A-E as defined on page 9

Load type	Maximum value during 30 minutes		
[MN] [MNm]	Exceedance probability 0.95	Most Probable	Exceedance probability 0.05
X-force	2.7	3.6	6.3
Y-force	0.6	1.0	2.5
Z-force	2.7	3.6	6.2
X-moment	0.6	1.7	7.4
Y-moment	4.0	7.5	20.0
Z-moment	0.5	1.0	2.5

Figure 1.8 Summary of estimated load level distributions for the accident condition, Hs = 4.0-4.1 m

2 Reaction forces on visor attachments

The possible distribution of reaction forces at the attachments of the bow visor has been studied by using equilibrium equations and assumptions of relative distribution and direction of forces.

2.1 Equations of equilibrium

The same direction of coordinates as used by SSPA is used here, i.e. x–forward, y–starboard and z–downwards. The origin of the system is placed at the deck hinge axis and CL-plane. Coordinates and notation of reaction forces are given in Figure 2.1 on the next page. In total 10 reaction forces at 5 different positions are considered.

The equations of equilibrium are formulated for 5 degrees of freedom, x-,z-forces and x-,y-,z-moments. Reaction forces in y-direction are not included because the levels of external y-forces (Fy) are relatively small, and because Fy are also possibly taken by the locating horns in addition to the attachments. However, the "yawing" Z-moment, (Mz) induced by external Fy is of importance and accounted for in the equations.

The "twisting" X-moment (Mx) about longitudinal axis is partly taken as y-, and partly as z-reaction forces at the attachments. Therefore, only half of Mx is considered in the equations below. This rough assumption is not critical for the results.

The lifting actuators are not considered to develop any reaction forces as long as the visor is kept in position by intact hinges and locks.

The equilibrium equations become:

x-forces: $(Rx_{hp}+Rx_{hs}) + (Rx_{sp}+Rx_{ss}) + Rx_a + Fx = 0$

z-forces: $(Rz_{hp}+Rz_{hs}) + (Rz_{sp}+Rz_{ss}) + Rz_a + Fz + W = 0$
(W is weight of visor)

x-moments: $(-Rz_{hp}+Rz_{hs})\cdot y_h + (-Rz_{sp}+Rz_{ss})\cdot y_s + Rz_a\cdot y_a + Mx/2 = 0$
(Mx/2 assumed taken by y-forces)

y-moments: $(Rx_{sp}+Rx_{ss})\cdot z_s - (Rz_{sp}+Rz_{ss})\cdot x_s + Rx_a\cdot z_a - Rz_a\cdot x_a + My - W\cdot x_g = 0$

z-moments: $(Rx_{hp}-Rz_{hs})\cdot y_h + (Rx_{sp}-Rx_{ss})\cdot y_s - Rx_a\cdot y_a + Mz = 0$

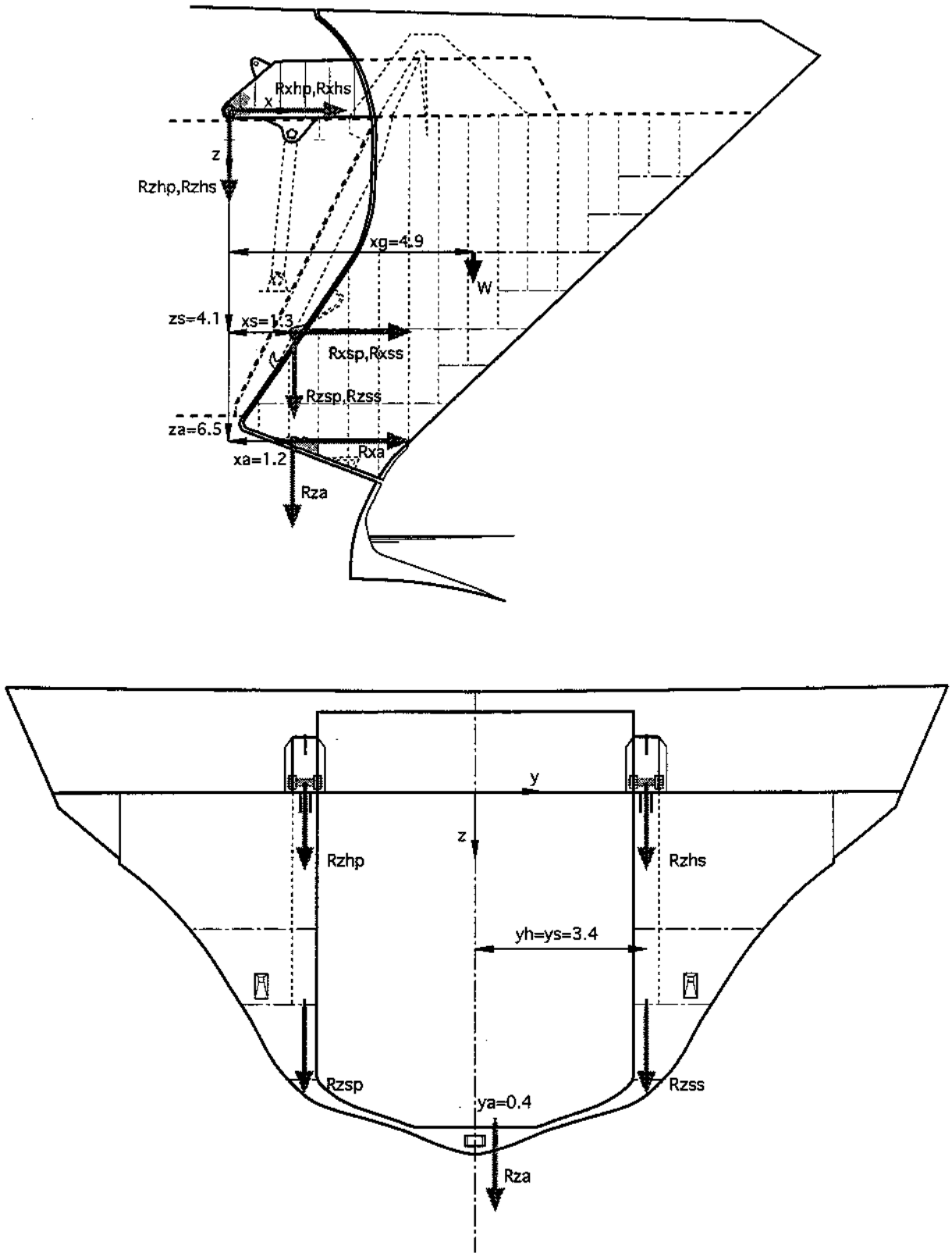

Figure 2.1 Coordinates and notation of reaction forces at attachments

2.2 Complementary equations

To solve for the ten unknown reaction forces it has been necessary to formulate five more conditions. Two are related to the geometry, and used here as fixed conditions. The direction of total reaction force in side locks and in the Atlantic lock have been assumed to be perpendicular to the hinge axis. This assumption is not critical since only the opening moment My is causing resultant tension in side and Atlantic locks.

$$(Rx_{sp}+Rx_{ss}) = -(x_s/z_s)\cdot(Rz_{sp}+Rz_{ss})$$

$$Rx_a = -(x_a/z_a)\cdot Rz_a$$

The last three conditions are related to to the stiffness and play in the system of attachments. They have been formulated as the relative distribution of moments taken by hinges and side locks for Mx and Mz, and by side locks and Atlantic lock for My. The influence of these conditions have been studied separately.

$$(-Rz_{hp}+Rz_{hs})\cdot y_h = (hsmx/(1-hsmx))\cdot(-Rz_{sp}+Rz_{ss})\cdot y_s$$

$$(Rx_{sp}-Rx_{ss})\cdot z_s - (Rz_{sp}-Rz_{ss})\cdot x_s = (samy/(1-samy))\cdot(Rx_a\cdot z_a - Rz_a\cdot x_a)$$

$$(Rx_{hp}-Rz_{hs})\cdot y_h = (hsmz/(1-hsmz))\cdot(Rx_{sp}-Rx_{ss})\cdot y_s$$

where hsmx = (Mx taken by hinges)/(Mx taken by hinges and side locks)
samy = (My taken by side locks)/(My taken by side locks and Atl. lock)
hsmz = (Mz taken by hinges)/(Mz taken by hinges and side locks)

2.3 Typical combinations of wave induced forces

The range of maximum wave force components considered has been covered by the following five typical cases A-E (also shown in Figure 1.7):

Load level:	A	B	C	D	E	
Resultant force:	3.9	5.2	6.5	7.9	9.2	[MN]
Components:						
Fx	-2.7	-3.6	-4.5	-5.4	-6.3	[MN]
Fy	0.6	1.0	1.5	2.0	2.5	[MN]
Fz	-2.7	-3.6	-4.5	-5.4	-6.3	[MN]
Mx	0.6	1.7	3.1	5.0	7.4	[MNm]
My	4.0	7.5	11.3	15.5	20.0	[MNm]
Mz	0.5	1.0	1.5	2.0	2.5	[MNm]

The different levels represent the estimated extreme value distribution in which level A has an exceedance probability of 95%, B is the most probable maximum and E has an exceedance probability of 5%. It is not certain that these force components will act simultaneously, but it is here considered as a sufficient assumption for the average conditions.

2.4 Results

The critical attachments in bow sea is the side lock on the wave encountered side, in this case the port side lock, and the Atlantic lock. The load carrying capacity of port side lock has been estimated by Rahka, VTT, to 1.2 MN, and the capacity of the Atlantic lock to 1.5 MN. However, calculations by Metsaveer, TTU, indicate the possibility of a significantly lower capacity for the Atlantic lock, somewhere in the range 0.8 - 1.4 MN dependent on the ultimate strength of the weldments. In the figures here is used a conservative assumption that the upper estimate is the critical value

The most critical of the complementary conditions is the percentage of opening moment My carried by side locks and Atlantic lock respectively. Figures 2.2-2.3 show the resultant reaction force in port side lock and Atlantic lock as function of the load level and the load distribution. When more than 40% of the opening moment is assumed taken by the side locks, the port side lock will be the first to fail. Due to the relative stiffer upper part of the visor and the high position of the wave forces centre of action, it is reasonable to assume that most of the opening moment will be taken by the side locks. Figure 2.4 shows an example of a critical load distribution assuming 67% of My carried by the two side locks, and Mx,Mz shared equally between hinges and side locks.

Figure 2.5 shows the influence of Mx, Mz distribution between hinges and side locks.

Figure 2.6 shows the influence of force centre of action. The moments My and Mz are varied by 20% with regard to the resultant force level. This variation is about the same as have been found from the model tests as shown in the previous Figure 1.7.

In conclusion, it can be estimated that the first failure of the port side lock will occur in a wave impact with a resultant force level of at most 7.0-8.5 MN. According to the previous estimate of wave load extreme value distribution, this corresponds to a failure probability of 10-25% during 30 minutes of exposure with a speed of 14.5 knots in a sea state with a significant wave height of 4.0–4.1 m.

Figures 2.7-2.8 show the reaction forces at starboard side lock and Atlantic lock when the port side lock has failed. It is not possible to ascertain which of the remaining locks that will be the second to fail. The capacity of the the starboard side lock has been estimated by different calculations to be at most 1.6 MN. It is also a possibility that the port side deck hinge will fail second due to the more downwards directed reaction force. In general the necessary wave load is about equal or slightly larger for any subsequent failure as for the initial failure. Figure 2.9 gives two examples of possible subsequent failure conditions after the port side lock has failed. The wave load level is here chosen as the same as in Figure 2.4.

2.5 Discussion

A reasonable accurate estimate of the relative stiffness of the visor and its attachments could only be obtained by a detailed finite-element analysis. However, since the play in the attachments and the actual distribution of dynamic wave pressure still would be undetermined, a FE-model is here judged to be of limited value.

The presented analysis is to bee seen as a qualitative illustration of the load distribution. All attachments are assumed working effectively and the wave load levels given for the initial failure is therefore possibly somewhat over-estimated. On the other hand, the analysis also shows that the necessary load level to fail the complete attachment system is not changing much even if one of the locks is considered ineffective or failed.

The failure sequence and approximately equal load level of initial and secondary failures are to some extent verified by the damage found at the various visor attachments of the near sister ship DIANA II in January 1993.

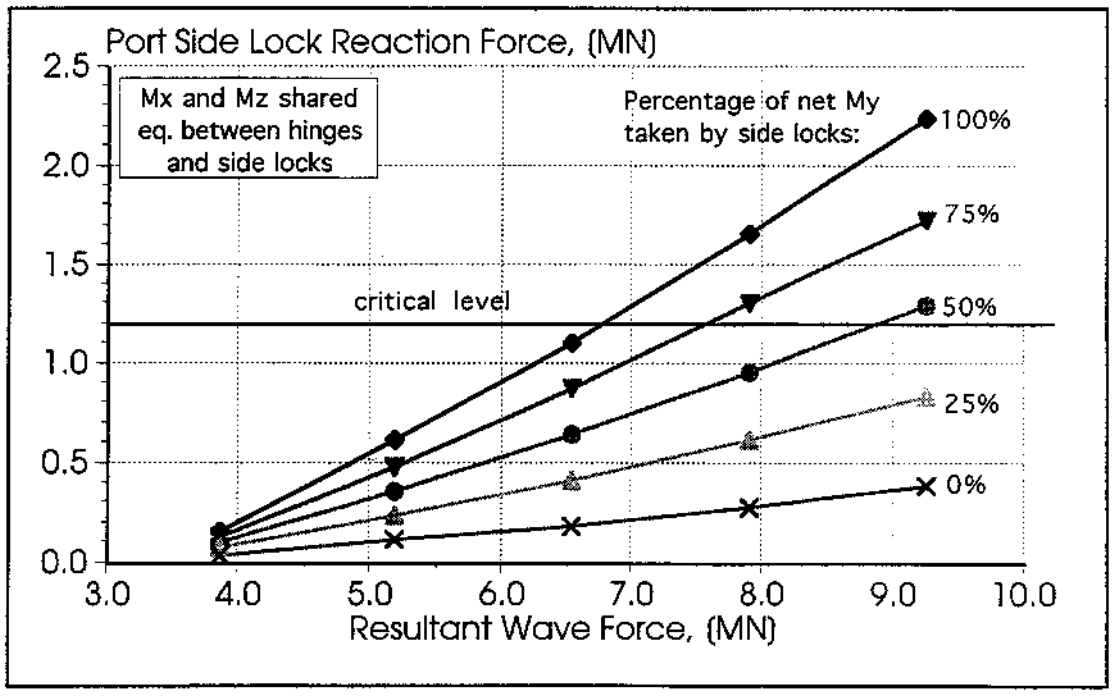

Figure 2.2 Port side lock reaction as function of wave force and My distribution between locks. All attachments intact

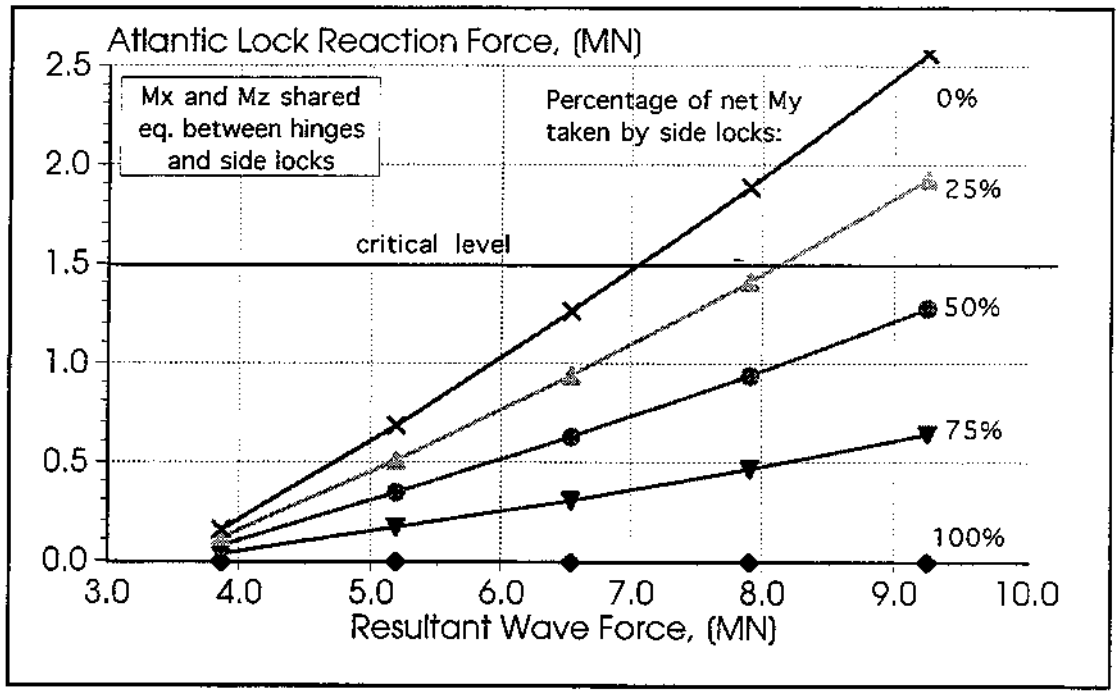

Figure 2.3 Atlantic lock reaction as function of wave force and My distribution between locks. All attachments intact

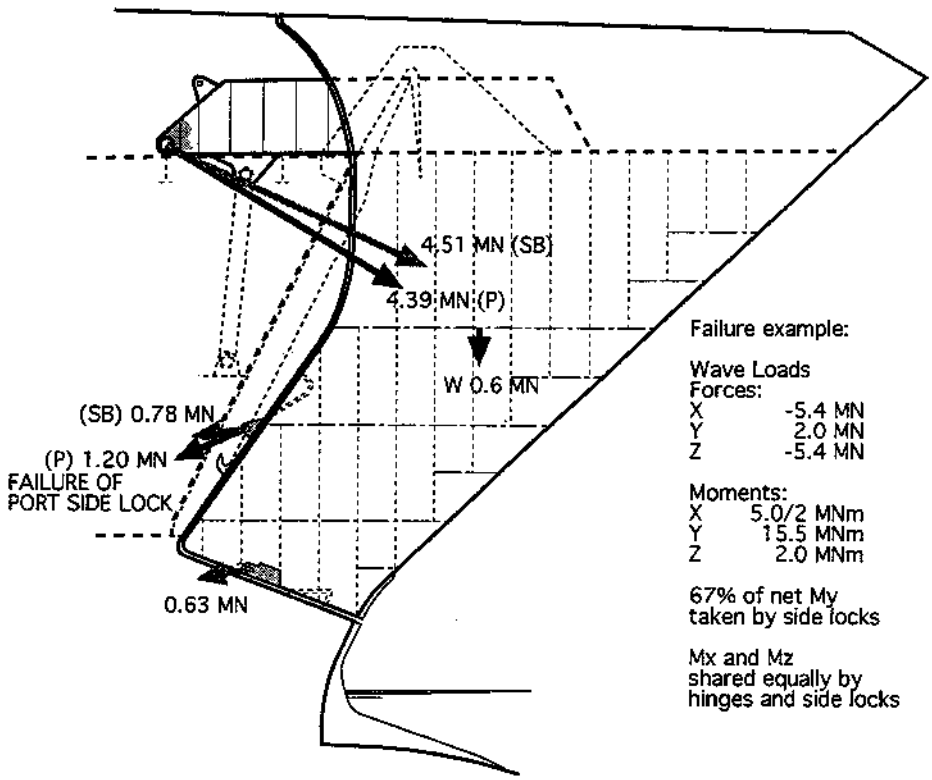

Figure 2.4 Example of reaction force distribution resulting in port side lock failure

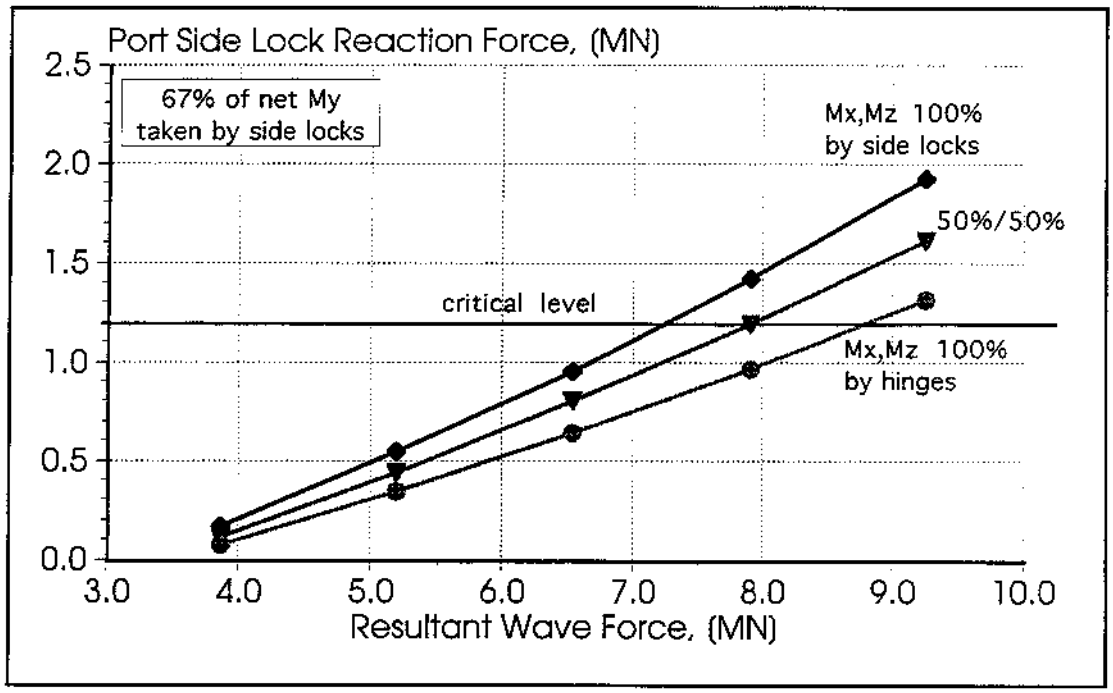

Figure 2.5 Example of influence from Mx,Mz distribution between hinges and side locks

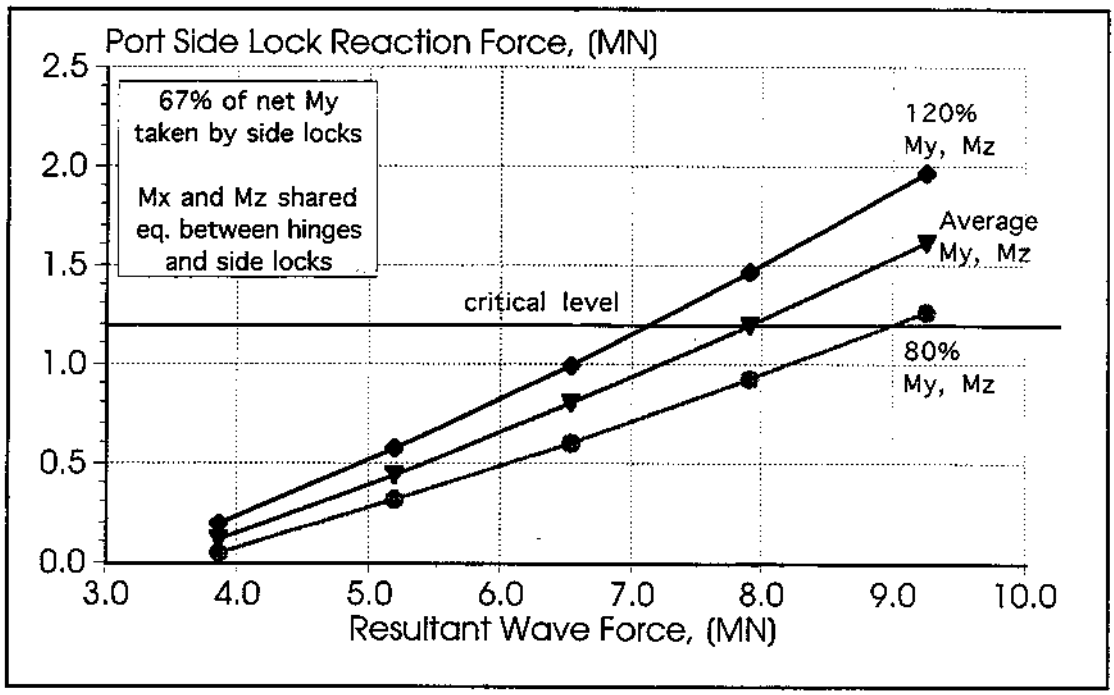

Figure 2.6 Example of influence from variation in My,Mz level

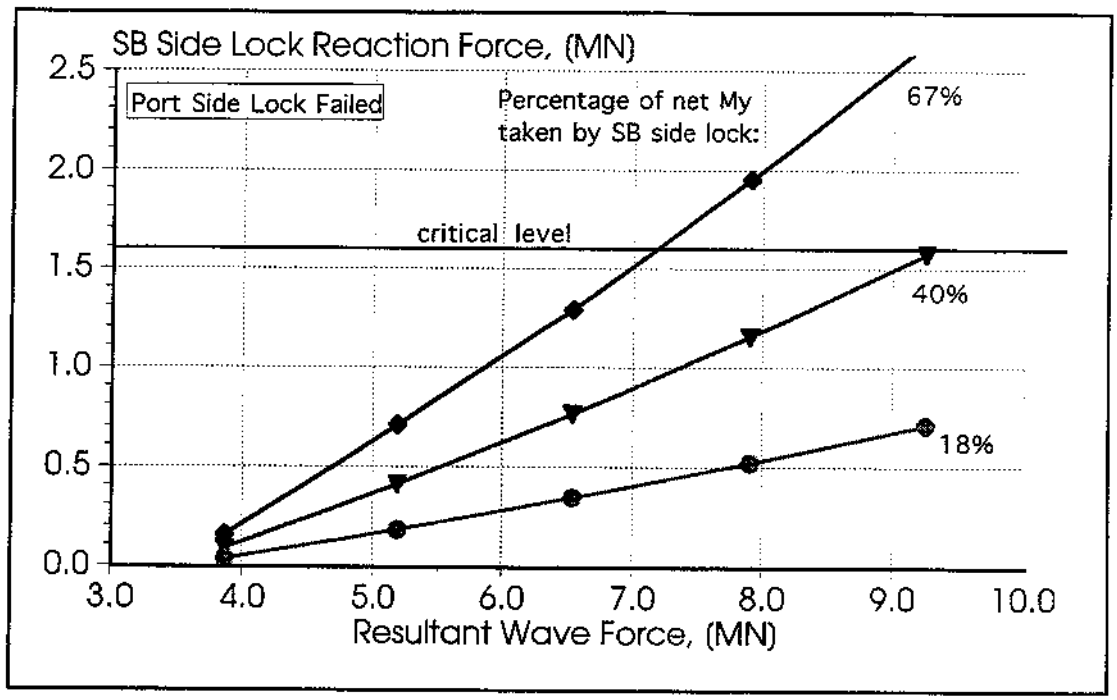

Figure 2.7 Reaction in starboard side lock after port side lock has failed

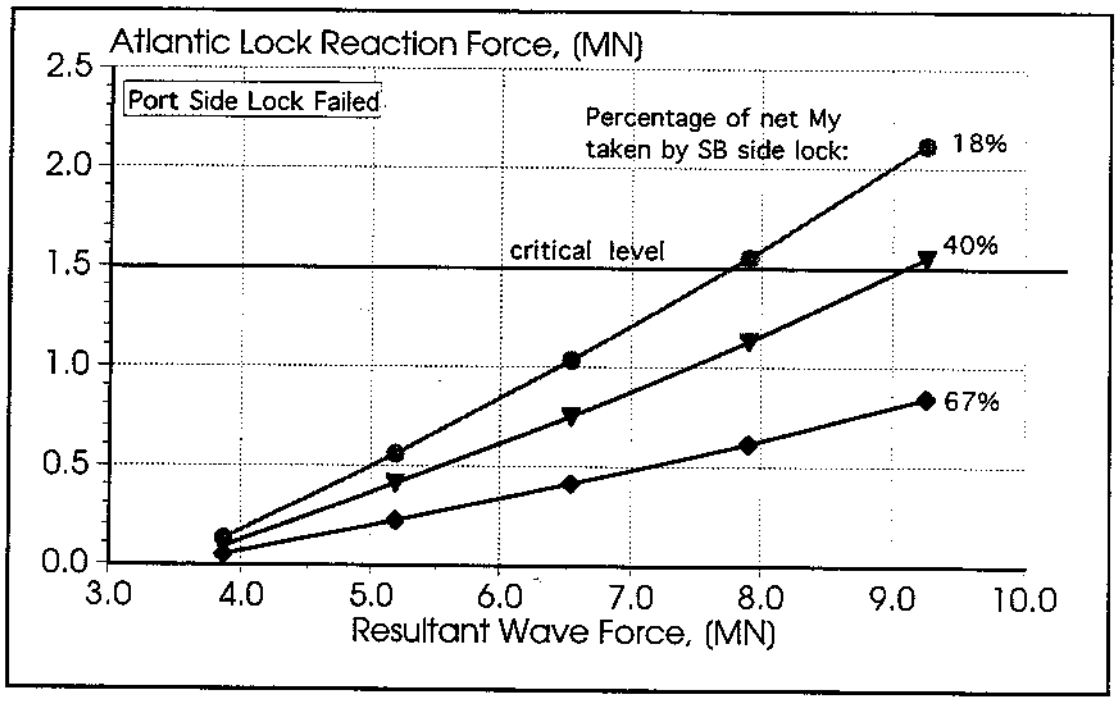

Figure 2.8 Reaction in Atlantic lock after port side lock has failed